International Journal of Innovative
Computing, Information and Control
Volume **12**, Number **6**, December **2016**

 ISSN 1349-4198
pp. 1989–2009

NOISE REMOVAL IN MONITORING SENSORS OF CIVIL STRUCTURES USING BLIND SOURCE SEPARATION

Daniel Moraes Santos and Antônio Claúdio Paschoarelli Veiga

Department of Electrical Engineering
Federal University of Uberlândia
Av. João Naves de Ávila, 2121, Uberlândia, Minas Gerais, Brazil
daniel.moraes@ufvjm.edu.br; acpveiga@gmail.com

Received April 2016; revised August 2016

Abstract. *Blind source separation (BSS) is known to be an efficient and powerful process to separate and estimate individual mutually independent signals acquired by various types of monitoring sensors. This paper proposes an algorithm to identify and reduce noise in monitoring sensor signals using blind source separation. This algorithm can be applied in any area of monitoring. It can identify noise without any kind of previous information of the signal analyzed. Initially, the algorithm makes the separation of the signals that were acquired by the sensors. These signals may have suffered influence from several noise sources. Different from the standard BSS, which requires at least two sources, this algorithm removes the noise from each signal separately applying the maximum signal-to-noise ratio and temporal predictability algorithms. The proposed algorithm also produces two outputs for each signal, the estimated original signal and the estimated noise. The results satisfy all the proposed objectives of this work. The proposed algorithm is a great solution for other types of applications, such as thermal profiling of wells.*
Keywords: Blind source separation, Statistical analysis, Sensors, Independent component analysis, Noise, Temporal predictability, Maximum signal noise ratio

1. **Introduction.** During the past years, there has been a major growth in the areas of construction [1], biomedicine [2] among other areas, both in Brazil and the world. With that, there has also been a very large demand on studies and researches to perform monitoring and/or signal acquisition in these areas. There are several types of sensors that perform these activities, for example, gauges [3] and accelerometers [4].

The resistive strain gauge has been the most used tool in experimental analysis of stress and deformation, since this instrument is one of the most accurate mechanisms in existence [5,6]. This type of sensor was chosen because it is very accurate. Since accurate sensor has low noise levels, it presents a great challenge for noise analysis. This device has wide applications in several areas, such as construction, aerospace, biomedicine, among others [7-10]. However, as this is a very sensitive device, it also captures multiple levels of noise, as temperature noise, Gaussian noise, among others [10-12].

The present research focuses on the problem of the noise present in the monitored signals. It aims to develop an algorithm that can be applied in general situations, detecting and reducing noise levels in the monitored signals. Such noise can be generated by different types of sources, both internal and external.

With so many areas of application for this type of algorithm, it was best to develop it in a generic way. In this way it can be applied in any area without the need to establish parameters for the input data. This makes it extremely practical.

To develop this algorithm, some technologies associated with this problem (noise) were analyzed. Since current active noise canceling technology itself produces noise, the ideal was to develop a different technology for noise reduction.

The BSS was used as a basis for being passive (no noise generation) and because of its ample applications. The BSS only uses statistical analysis, requires no parameters of the input variables, and does not need any kind of prior knowledge of the monitored signal [13,14].

Zarzoso and Nandi [15] performed comparative tests between noise reduction techniques. BSS and adaptive noise cancellation techniques were used in this comparison. Their experimental results demonstrated the more robust performance of the BSS technique, which confirms the validity of this technique as a great solution for noise reduction. Thus, the proposed algorithm is using a well-established technology for this type of application.

The statistical analysis carried out by the BSS is based on the independent component technique, which performs the separation of independent variables very effectively [16]. According to He et al. [17], independent component analysis is very efficient in the treatment of noise. The technology chosen by the proposed algorithm is based on this feature, because the signal analyzed is made of random variables (noise).

Ferdjallah and Barr [18] presented a solution for noise reduction on monitored signals that also uses active filters. They reported that this type of technique is not a universal solution for such problems. The proposed algorithm performs noise reduction, both captured by sensors as well as those generated by the monitoring equipment. This process of noise reduction is done statistically, i.e., without using any electronic equipment, avoiding the generation of more noise. It also presents itself as a universal solution for any application in noise reduction, since it does not need any input parameter of the analyzed signal.

Clansy et al. [19] mentioned that in EMG monitoring equipment (electromyography) there are problems in the acquisition of the signals. These problems may be present in the materials used in the sensors, which may not present the same characteristics, or in possible calibration problems of the equipment. Therefore, they would acquire signals with small distortions. To solve such problems, he suggests the use of digital filters and adaptive filters as techniques for reduction of these noises. Once again we have the problem of the presence of noise. However, the technology applied still uses electronic components, which themselves produce noise.

Many researchers are interested in the area of reduction of noise. Therefore, there is a very large amount of research proposing several solutions. These solutions increasingly tend to use techniques that do not make use of electronic circuits [15-17,20]. The proposed algorithm also follows this technological evolution.

The problem of noise also occurs in the monitoring of structures, as it also uses electronic equipment that uses sensors. However, this work presents a noise reduction technique that does not insert other types of noise generated by the use of electronic components.

There is a growing demand for techniques that monitor structures, as most existing ones are not effective in the early stages of damage [21]. Thus, the proposed algorithm is justified in that it presents a new technique to perform noise reduction of signals in monitored structures. With more accurate signals it is possible to detect damage in early stages. At this stage the signals have small amplitude (small variations); thus, any level of noise removed is of great importance for the efficiency of the signal analyzed.

The technique chosen for the proposed algorithm is also justified by the growing study of noise reduction in the process of acquisition of signals in real time [19,22], since it has low computational complexity [13].

The proposed algorithm, being validated using precise sensors that are less sensitive to noise, such as gauges [3], can be used in applications whose sensors are more sensitive to noise, as in probes for monitoring wells, of small or great depth.

The big problem and one of the biggest constraints of signal acquisition, as in all types of sensors, is the inherent noise level derived from various sources, such as Gaussian and temperature noise, and even the mixing of signals between sensors. This problem has been researched for a long time by specialists of the area [23].

In addition to noise that can be inserted in the signals by the acquisition equipment, there is also the lack of efficiency of noise reduction from signals obtained from sensors. This raises the possibility that the signals used as monitoring parameters may not be completely free of noise, in spite of the fact that most equipment uses active noise reduction systems (filters) [24].

The proposed algorithm only uses techniques purely based on the statistical analysis of signals, which do not generate noise, as is desired [25-28]. Blind source separation (BSS), has recently received attention in the fields of signal processing and neural networks because of its potential in various applications, such as wireless communication, speech recognition, and biomedical signal processing [29].

BSS processes and analyzes the data, in order to recover, acknowledge or separate unknown sources solely from the signals obtained by a set of sensors [13]. It does not need the input of parameters or data modeling, thus making it a very powerful tool for such activities [14].

This technique is based on some statistical theories, such as independent component analysis (ICA) and principal component analysis (PCA), performing a purely statistical separation of signals [25,30-32].

The proposed algorithm used two sets of signals for analysis and validation. The first set consists of two signals generated through the readings of gauges 1 and 2, monitoring the same point in a practical experiment. The second was also composed of two signals. One signal was acquired by a strain gauge on a practical experiment. The other was a signal generated through a mathematical model using finite elements [33], simulating the behavior of the practical experiment conducted [34].

To analyze the results, we used the signal-to-interference model (SIR) [35], the signal-distortion ratio (SDR) and signal-to-noise ratio (SNR) [36] and the convergence of signals (experimental signal, mathematical signal and BSS signal).

For the process of acquisition of signals in any kind of monitoring various sensors are positioned in different locations, with the purpose of obtaining the behavior of the structure. When sensors are positioned close to each other, part of the signals acquired by each sensor suffers interference from neighboring sensors, thus causing interference in the signals.

The BSS performs the separation of the signals monitored, which could have been mixed in the acquisition process. When performing the statistical recovery of each signal, the parts of the signal of neighboring sensors, which are considered noise, are removed and relocated to the correct sensors. In this way, it ceases to be considered noise, and becomes a part that completes the monitored signal in each sensor [13,14].

The problem that can occur is that the BSS needs at least two sensors to perform the separation of interference between them [30-32]. This is a very important problem. It becomes impossible to perform the analysis of some signals in specific applications, as for example, the monitoring of a single probe temperature, moisture, and PH.

The proposed algorithm solved this problem, operating with only one input signal and poducing two output signals. The first output signal is the monitored signal with considerably reduced noise and the second is the noise removed from the monitored signal.

Thus, the proposed algorithm can be implemented using only one input signal and producing two signals after processing. The proposed algorithm identifies and removes levels noise from the signals analyzed. The BSS only performs the separation of mixed signals [30-32].

The traditional noise filtering systems also have the problem of not being able to characterize noise signals. They only can, at most, determine the average energy of the signal [37]. Since the proposed algorithm produces separate signal and noise outputs, it is capable of detecting and characterizing the behavior of the noise levels present in signals monitored.

With all these functionalities, the proposed algorithm achieved its goal of having a wide and simple application in virtually all areas that require monitoring.

In the following sections we will present, with details, the methods used, the experimental conditions, the tests and the results.

The following presents all the symbols and notations used in this work.
BSS: Blind source separation;
ICA: Independent component analysis;
PCA: Principal component analysis;
SIR: Signal-to-interference ratio;
SIR^{in}: Signal-to-interference ratio before application of the algorithm;
SIR^{out}: Signal-to-interference ratio after application of the algorithm;
$SIRI$: Signal-to-interference ratio average;
SDR: Signal-distortion ratio;
SNR: Signal-to-noise ratio;
S: BSS Input signals;
A: BSS Mixture matrix;
X: Mixed input signals with noise added;
V: Noise signals used in the BSS;
W: BSS unmixing matrix;
Y: Input signals estimated by BSS;
X_i: Proposed algorithm input signals;
$X_{i\,Displaced}$: Input signals of the proposed algorithm with time delay;
Short cable: 5-meter long cable used in practical monitoring;
Long cable: 30-meter long cable used in practical monitoring;
Staright cable: cable laid in rectilinear form used in practical monitoring;
Curled cable: cable laid in coiled form used in practical monitoring;
F: Cost function used by BSS;
$\widetilde{\boldsymbol{y_\tau}}$: Short term moving average of temporal predictability algorithm;
$\overline{\boldsymbol{y_\tau}}$: Long term moving average of temporal predictability algorithm;
h_L: Term half-life;
λ_L: Lambda of long term moving average;
λ_S: Lambda of short term moving average;
$\bar{C}$: Matrix of long-term covariances;
$\tilde{C}$: Matrix of short-term covariances;
S_j: Original signals adopted by the performance algorithm;
$\hat{S}_j$: Estimated signs adopted by the performance algorithm;
S_{target}: Modified version of the original signals used by the performance algorithm;
e_{interf}: Interference error;
e_{noise}: Noise error;
e_{artif}: Artifact error;

P_{S_j}, P_S, $P_{S,V}$: Orthogonal projectors;
H: Hermitian transpose;
$\boldsymbol{R}_{SS}$: Gram matrix;
PDF: Gaussian probability density function;
pn: The fundamental structure of the electronic components commonly called semiconductors;
i: Instantaneous current;
i_D: Current average value;
$\overline{i_S^2}$: Shot noise;
$\overline{e_T^2}$: Thermal noise;
$\overline{e_F^2}$: Flicker noise;
δ: Standard deviation (shows how much dispersion exists relative to the mean);
δ^2: Variance (shows the distance, in general, between the values and the expected values);
RMS: A statistical measure of the magnitude of a variable amount.

2. **General Configuration of the BSS.** Blind source separation (BSS) aims to estimate individual mutually independent signals by observing signals acquired by sensors. This separation is essential when working with sources that are mixed by an unknown model and only mixed signals are available from the sensors. This technique is called blind because the estimate is performed without any prior knowledge of the original sources, or of the model used in the mixture [38].

The lack of prior information of the sources should not be understood as something negative for the model. On the contrary, it is a big advantage in this case, since it makes it a versatile tool in the exploration of diversity generated by the number of sensors used [39].

To define the problem of BSS, consider, initially, the template for the solution to the problem of blind signal processing shown in Figure 1, where it admits that a certain number of signals, determined by the equation $S = [S_1, S_2, \ldots, S_n]^T$, is being sent, or transmitted by any physical source through a channel A.

The signals, determined by the equation $X = [X_1, X_2, \ldots, X_m]^T$, in addition to being mixed with signals from different sources, suffer the influence of noise and interference $V(k)$.

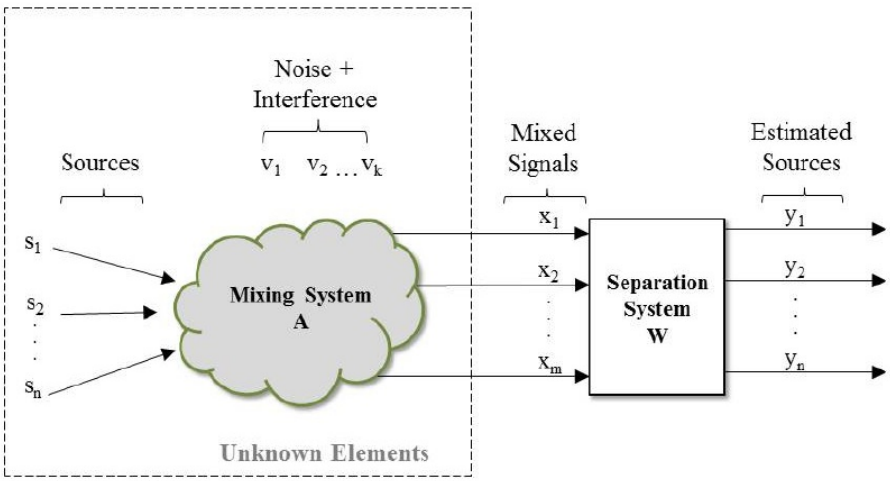

FIGURE 1. Variables, steps and development of BSS pattern

The problem of blind signal processing is finding the original signals S from the sensor measurements X. The solution is to extract the original signals from the mixture through a system W to provide an estimate of these signals given by $Y = [Y_1, Y_2, \ldots, Y_n]^T$.

In the most general case handled by blind signal processing, we consider m mixed X signals. These signals are combined linearly from n source signals S, and from channel A, which is an m by n matrix. In general, we have that $m > n$, and the presence of noise is given by $V = [V_1, V_2, \ldots, V_n]^T$. The mathematical formulation of the system shown in Figure 1 is characterized by $X = AS + V$ and $Y = WX$.

A consideration regarding the mixing system is given to the presence or absence of noise. The definition of noise is always problematic. Therefore, there are basically two ways to consider its presence in the system [13]. The first deals with noise as a source to be separated from the others. It is picked up by the sensors in the same way of the other sources [25,40]. The other approach treats noise as an element that decays and mixes and, therefore, cannot be recovered [41-43]. Figure 1 describes this last consideration.

3. **Proposed Algorithm.** Initially, we apply the BSS to signals sampled by standard sensors for monitoring civil structures, identified by vector X, being composed by the mixture of parts of the signals from each sensor plus a noise level, given by $V = [V_1, V_2, \ldots, V_n]^T$.

Most of the equipment currently used to perform the monitoring of signals cannot eliminate noise levels present in the reading of the sensors. In fact, this equipment may even add some type of noise to the signals, since most of it uses noise reduction systems based on active filters (electronic noise).

In this first stage, it is assumed that the noise is inherent to the signal as mentioned previously [41-43], and cannot be separated from the signal. Thus we obtain only the number of signals corresponding to the same amount of sensors used in monitoring, that is, the vector size S is the same as the vector Y as shown in Figure 1.

In the second stage of the proposed algorithm, the application of the BSS is different from standard applications, as in the first stage. The BSS is applied to each input signal, to each individual sensor (first to X_1 only, then to X_2 only, and so on, and not to the whole vector X), of a monitoring system. In this stage, the outputs from the first stage are considered as inputs to the BSS, which are signals estimated to have noise.

Unlike the standard BSS, the algorithm proposed uses a single input signal mentioned above. This signal is shifted in time n units; thus, the second input signal. The BSS algorithm is applied to these two input signals, thus generating two outputs, Y and V. The first is the estimated signal with considerably reduced noise and the second is the noise present in the signal X shown in Figure 2.

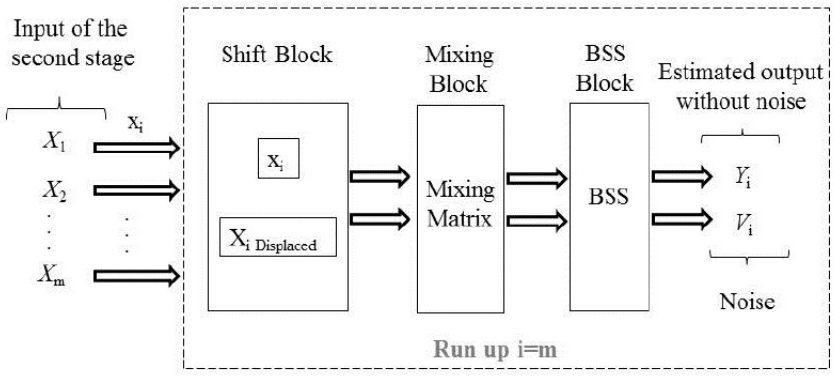

FIGURE 2. Architecture of the proposed algorithm based on BSS technology

As stated earlier, the analysis is done on separate signals, which can be applied when the monitoring system has only a single sensor, or several sensors far apart, resulting in almost zero interference between sensors. Then we may consider that in each signal there is only the desired signal and unwanted noise, and discard the first stage of the proposed architecture.

Figure 2 identifies the proposed algorithm input signals as "second-stage input". It is considered that the monitored signals were processed by the BSS algorithm. However, these monitored signals may be completely independent from one another.

As an initial step the proposed algorithm analyzes the first signal (X_1). n samples are delayed in time, creating a second signal ($X_{1\,Displaced}$), having as reference the analyzed signal (X_1).

After this step, the two signals (X_1) and ($X_{1\,Displaced}$) are mixed using a random mixing matrix (A). This step is necessary because the BSS can only be applied to a mixed signal. In the third step the BSS algorithms (temporal predictability and maximum signal noise ratio) are applied to the two mixed signals. The number of outputs of the BSS is exactly equal to the number of inputs. The two input signals are practically the same, (X_1) and ($X_{1\,Displaced}$) with a temporal offset of n samples. One output is the signal X_1 with reduced noise and the other is the noise removed from the output signal X_1.

In the last step, the probability density function of the noise is determined by the proposed algorithm. This is done to verify if the noise signal has a Gaussian density.

These steps are repeated until all monitored signals are analyzed, i.e., until $i = m$.

We used the data acquisition system [44] with half-bridge configuration [6] for conducting the tests. The comparison parameter used was the signal-to-noise ratio of the same equipment [44], but from its most current version [45] that features an SNR of 7 dB.

4. **Theoretical Noise Level.** Currently there are several definitions of noise. The relevant noise definition for this work is: any unintentional fluctuation that appears at the top of the signals to be measured. In electronic circuits there are voltage and current noise caused by thermal fluctuations of the components [46]. There are several types of noises that interfere with signals analyzed when electrical equipment is used to perform monitoring [10-12].

For example, shot noise is always associated with a current flow. It appears whenever a load is going through a potential barrier, such as a pn junction. This is a purely random event. Thus, the instantaneous current i is composed of a large number of random and independent current pulses, with average value i_D. Shot noise is usually specified in terms of the square of its average variation over its average value [47]. This is described by Equation (1):

$$\overline{\iota_S^2} = \overline{(\iota - \iota_D)^2} = \int 2q_i df \tag{1}$$

where q is the electron charge and df is the variation in frequency. This type of noise has a uniform density of energy.

Thermal noise is caused by the thermal agitation of the charge carriers (electrons or holes) in a conductor. This noise is present in all passive resistive elements. This type of noise also has a uniform density of energy, but is independent of the current flow [47]. The value of the square of the mean of the noise source of voltage or current is calculated by Equation (2):

$$\overline{e_T^2} = \int 4KTRdf \text{ or } \overline{\iota^2} = \int \frac{4KT}{R} df \tag{2}$$

where K is the Boltzmann constant ($1.38 * 10^{-23}(j/K)$), T is the absolute temperature in Kelvins (K), R is the resistance in Ohms of the physical means and df is the variation

in frequency. The terms $4KTR$ and $4KT/R$ are energy densities of voltage and current, with units of V^2/Hz and A^2/Hz.

Since the noise sources have amplitudes, which vary randomly over time, they can only be specified by a probability density function. Thermal noise and shot noise have Gaussian probability density functions. Be δ the standard deviation of the Gaussian distribution, by definition, δ^2 (variance) is the variation of the square of the average over the average value. This means that noise signals with Gaussian distribution, the average square variation over the mean value, i^2 or e^2 is the variance δ^2, and the RMS value is the standard deviation δ [47].

Theoretically, the amplitude of the noise can have values approaching infinity. However, the probability decreases rapidly with increase in amplitude. An effective limit is $\pm 3\delta$, since the magnitude of the noise is within that limit 99.7% of the time. Figure 3 shows graphically how the probability amplitude relates to the RMS value [47].

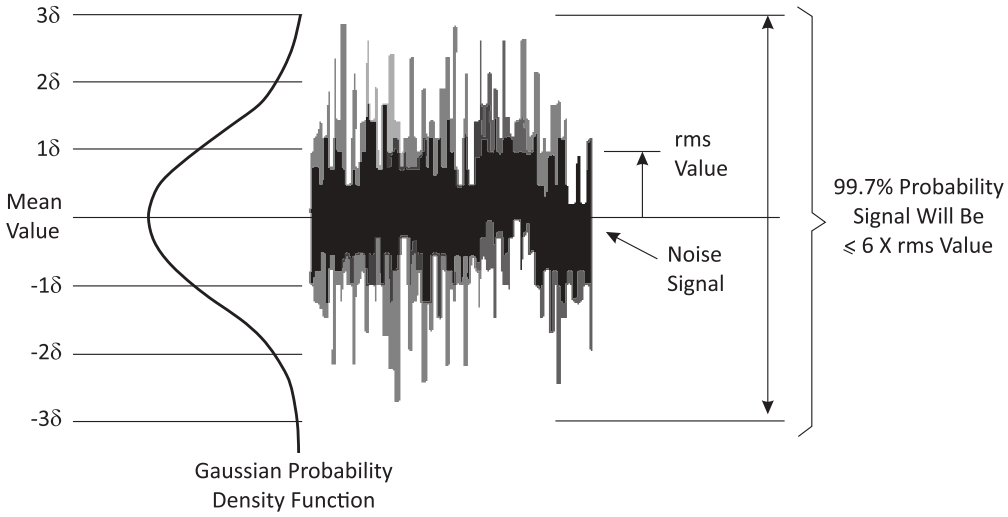

FIGURE 3. Behavior of the Gaussian probability density function with variables: RMS, mean values and standard deviation [38]

With several sources of noise in a circuit, the signal must be properly combined to get the signal from the noise. For purposes of analysis, let us consider two noise sources combined (there may be numerous noise sources). Each has an associated noise generator as shown in Equation (3) [47]:

$$\overline{e_1^2} = \int 4KTR_1 df \text{ and } \overline{e_2^2} = \int 4KTR_2 df \tag{3}$$

To calculate the square of the average tension, $\overline{E_t^2}$, through these two sources, let $E_t(t) = e_1(t) + e_2(t)$ be the instantaneous value [47]. So,

$$\overline{E_t(t)^2} = \overline{[e_1(t) + e_2(t)]^2} = \overline{e_1(t)^2} + \overline{e_2(t)^2} + \overline{2e_1(t)e_2(t)} \tag{4}$$

Since the noise tensions, $e_1(t)$ and $e_2(t)$, come from different sources, they are independent, and the average of their product is zero [47],

$$\overline{2e_1(t)e_2(t)} = 0 \tag{5}$$

The result is:

$$\overline{E_t^2} = \overline{e_1^2} + \overline{e_2^2} \tag{6}$$

So, as long as the noise sources originate from separate mechanisms and are independent, which usually occurs, the square of the mean value of the sum of separate and independent noise sources is the sum of the squares of the individual average values [47].

For the characterization of noise to be precise a lot of information is necessary, such as the probability density function of the noise. However, it is not always possible to know this information in detail. The operation of the proposed algorithm is based on the Chebyshev inequality [37].

The standard deviation δ_x of a random variable x is a measure of the size of its probability density function. The higher the δ_x, the wider is the probability density function. Figure 4 illustrates this effect for a Gaussian probability density function [37].

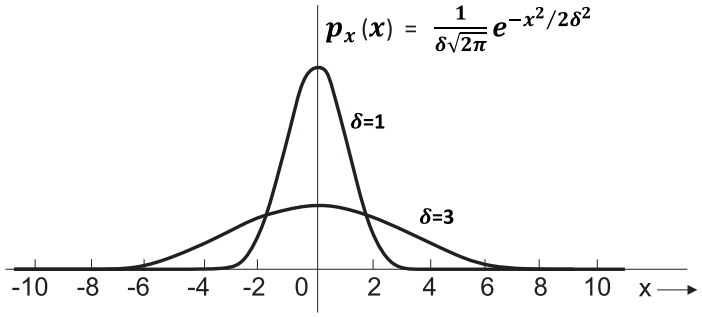

FIGURE 4. Gaussian PDF with standard deviation $\delta = 1$ and $\delta = 3$ [41]

The Chebyshev inequality is a proof of this fact. This can be verified in Equation (7) [37],

$$P[|X - \mu| < K\delta] \geq 1 - \frac{1}{K^2} \leftrightarrow P[\mu - K\delta < X < \mu + K\delta] \geq 1 - \frac{1}{K^2} \tag{7}$$

With $K = \pm 3\delta$ there is a probability of more than 99% that the amplitude of the signal will be within that range.

The direct calculation of probability involving Gaussian distribution requires capabilities of infinitesimal calculus, and even so, given the shape of the probability density function, it is not a simple process. So, these calculations were put in a table, allowing us to obtain the desired probability value directly [48].

The Gaussian density function depends on two parameters, μ and δ (mean and standard deviation, respectively), so that, if the probabilities were put in a table directly from this function, double-entry tables would be necessary, complicating things considerably. Therefore, a change of variable was made. Random variable X was defined as random variable Z through [48]:

$$Z = \frac{X - \mu}{\delta} \tag{8}$$

This new variable is called normal standardized variable. Its average is zero, and its standard deviation is 1 [48].

The determination of parameters in relation to noise is confined to the calculation of average values through probability density functions. The exact specification of the punctual value of amplitude of the noise cannot be determined theoretically. With this, the contributions made by the proposed algorithm become even clearer and decisive for the study. It contributes considerably to the characterization of noise in signals monitored by electronic equipment. This is because the proposed algorithm can estimate the noise and separate it from the monitored signal.

The proposed algorithm considers the noise present in this type of monitored signal as a Gaussian probability density function.

5. **Signals Analyzed.** Some experiments and laboratory analyses were performed to have enough data to develop a thesis about the reduction of noise even after the output from the acquisition equipment.

The first experiment was performed using two resistive strain gauges of 5 mm each, monitoring the same point of deformation. They were set side by side so that they could monitor the same angle of deformation of a specific point of a platform.

For each strain gauge two lengths of cables were used, one with 5 meters and the other with 30 meters. The way these cables were set was also alternated, straight and curled. One test was made where we used a moving magnet within the curled 30-meter cable.

All of the settings of these tests were carried out in order to generate different noise levels at each input of the equipment. If the equipment has an efficient noise reduction system, the output signals will have practically the same values in all cases, and consequently, the proposed algorithm will find a null noise level in the output of the signals.

The signals used in the first input set are described in Figure 5, describing the variations of each strain gauge analyzing the same point of reference.

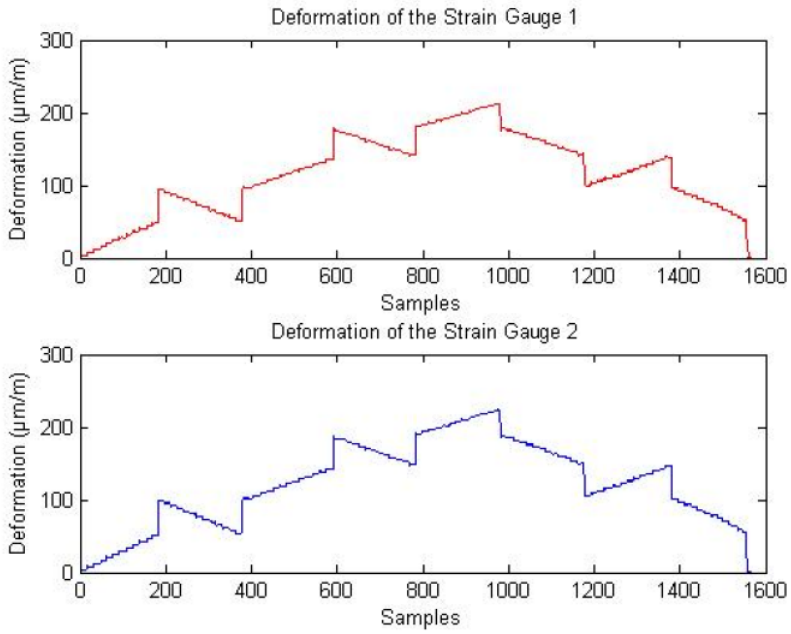

FIGURE 5. Deformation signals monitored during the implementation of the practical experiment using two gauges

6 tests were executed, using the possible configurations with the variations mentioned previously, as shown in Table 1.

The second set of input signals used by the proposed architecture is described in Figure 6, describing the signal of the practical experiment conducted in the laboratory, and its corresponding signal, determined by the numerical model [34] built using finite elements [33].

6. **Maximum Signal-to-Noise Ratio Algorithm.** The blind source separation algorithm is based on the characteristic that signal-to-noise ratio (SNR) is maximum when statistically independent source signals are completely separable. Source signals are replaced by moving average estimated signals. The function of covariance matrices of the signals and noise sources is expressed by the widespread problem of eigenvalues, and the

TABLE 1. Configuration of the physical parameters of the practical experiments versus theoretical noise levels

Test Number	Equipment Input	Cable Length		Cable Layout		Theoretical Noise Level
		Short	Long	Straight	Curled	
Test 1	Strain Gauge 1	X			X	Greater
	Strain Gauge 2	X		X		Minor
Test 2	Strain Gauge 1	X			X	Minor
	Strain Gauge 2		X		X	Greater
Test 3	Strain Gauge 1	X		X		Minor
	Strain Gauge 2		X		X	Greater
Test 4	Strain Gauge 1	X		X		Minor
	Strain Gauge 2		X	X		Greater
Test 5	Strain Gauge 1[1]		X		X	Greater
	Strain Gauge 2	X		X		Minor
Test 6	Strain Gauge 1		X	X		Minor
	Strain Gauge 2		X		X	Greater

[1]Test performed with a magnet moving within the curled cable.

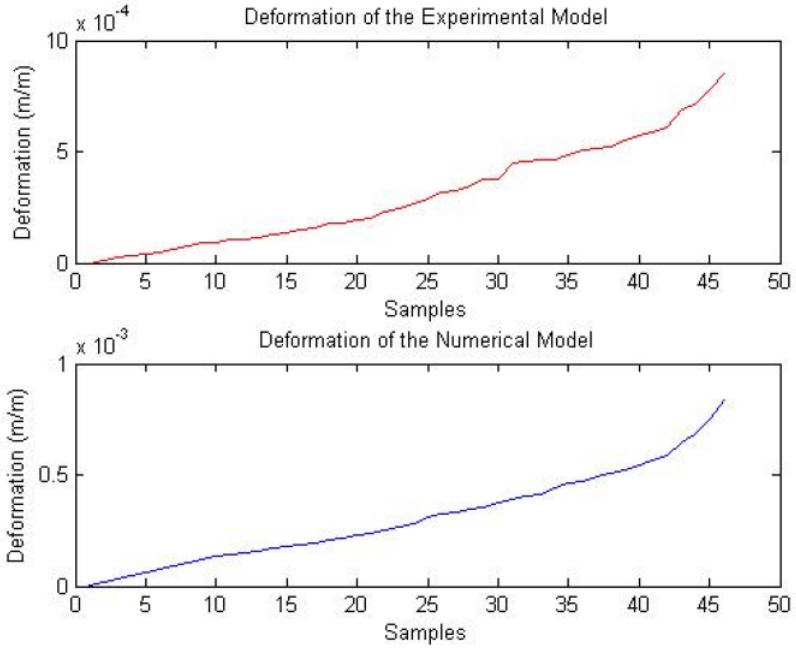

FIGURE 6. Deformation signals of the experimental and numerical models [36]

unmixing matrix was developed to address the widespread problem of eigenvalues without any interactivity [49]. Thus, low computational complexity is applied.

Some authors have stated that the temporal predictability of a mixed signal is not always smaller or equal to its source signals. With that in mind, this work also performed the maximum signal-to-noise ratio algorithm, which is defined by a signal-to-noise ratio function [29].

According to the blind source separation model, the error between the original signals and the estimated signals is considered as noise, so the formula of the signal-to-noise ratio

is

$$SNR = 10\log\frac{s\cdot s^T}{e\cdot e^T} = 10\log\frac{s\cdot s^T}{(s-y)\cdot(s-y)^T} \tag{9}$$

The original $\boldsymbol{s}$ signals are unknown. Therefore, a moving average of the $\tilde{\boldsymbol{y}}$ signals is used instead of the original $\boldsymbol{s}$ signals. Consequently Equation (9) can be rewritten,

$$SNR = 10\log\frac{s\cdot s^T}{e\cdot e^T} = 10\log\frac{\tilde{\boldsymbol{y}}\cdot\tilde{\boldsymbol{y}}^T}{(\tilde{\boldsymbol{y}}-y)\cdot(\tilde{\boldsymbol{y}}-y)^T} \tag{10}$$

where $\tilde{\boldsymbol{y}}(n) = \frac{1}{p}\sum_{j=0}^{p}\boldsymbol{y}(n-j)$ is the moving average of the $\boldsymbol{y}$ signals, p integer is the size of the moving average (p less than 100). To simplify the calculation, $\tilde{\boldsymbol{y}}$ in the numerator is replaced by $\boldsymbol{y}$. The maximum signal-to-noise ratio cost function is defined as:

$$F(\boldsymbol{y}) = SNR = 10\log\frac{\boldsymbol{y}\cdot\boldsymbol{y}^T}{(\tilde{\boldsymbol{y}}-y)\cdot(\tilde{\boldsymbol{y}}-y)^T} \tag{11}$$

where $\boldsymbol{y} = \boldsymbol{W}\boldsymbol{x}$, $\tilde{\boldsymbol{y}} = \boldsymbol{W}\tilde{\boldsymbol{x}}$, where $\tilde{\boldsymbol{x}}$ is the moving average mixture signals $\boldsymbol{x}$, given by

$$\tilde{\boldsymbol{x}}(n) = \frac{1}{p}\sum_{j=0}^{p}\boldsymbol{y}(n-j) \tag{12}$$

Optimizing the cost function, Equation (11) can be rewritten [29],

$$\begin{aligned} F(\boldsymbol{W},\boldsymbol{x}) &= 10\log\frac{\boldsymbol{y}\cdot\boldsymbol{y}^T}{(\tilde{\boldsymbol{y}}-y)\cdot(\tilde{\boldsymbol{y}}-y)^T} = 10\log\frac{\boldsymbol{W}\boldsymbol{x}\cdot\boldsymbol{x}^T\boldsymbol{W}^T}{\boldsymbol{W}(\tilde{\boldsymbol{x}}-\boldsymbol{x})\cdot(\tilde{\boldsymbol{x}}-\boldsymbol{x})^T\boldsymbol{W}^T} \\ &= 10\log\frac{\boldsymbol{W}\bar{\boldsymbol{C}}\boldsymbol{W}^T}{\boldsymbol{W}\tilde{\boldsymbol{C}}\boldsymbol{W}^T} = 10\log\frac{\boldsymbol{V}}{\boldsymbol{U}} \end{aligned} \tag{13}$$

According to Equation (13), derivative F in relation to $\boldsymbol{W}$ is,

$$\frac{\partial F}{\partial \boldsymbol{W}} = \frac{2\boldsymbol{W}_i}{V_i}\bar{C} - \frac{2\boldsymbol{W}_i}{U_i}\tilde{C} \tag{14}$$

The gradient of the derivative F in function of $\boldsymbol{W}$ is zero, obtaining Equation (15) [29,43],

$$\boldsymbol{W}_i\bar{C} = \frac{V_i}{U_i}\boldsymbol{W}_i\tilde{C} \tag{15}$$

The results presented in this article were obtained using the eigenvalue function of Matlab, being $\boldsymbol{W} = \boldsymbol{eig}\left(\bar{C},\tilde{C}\right)$. All the K can be then estimated by $\boldsymbol{y} = \boldsymbol{W}\boldsymbol{x}$, where each line of $\boldsymbol{y}$ corresponds exactly to one estimated $\boldsymbol{y_i}$ signal, as in the algorithm of temporal predictability.

7. **Algorithm of Temporal Predictability.** The measure of temporal predictability is defined and used to separate signals from linear mixtures. For any set of signals from statistically independent sources we have the property: The temporal predictability of any mixed signal is less than, or equal to any one of its original source signals. This shows that this property can be used to retrieve the source signals from a set of linear mixtures of these signals. This property determines an unmixing matrix that maximizes the value of Temporal Predictability for each recovered signal. This matrix is obtained as the solution for the problem of eigenvalue [50].

Consider a set K of statistically independent sources signals $\boldsymbol{s} = (S_1, S_2, \ldots, S_k)^T$. A set of $M \geq K$ linear signal mixtures $\boldsymbol{x} = (X_1, X_2, \ldots, X_M)^T$ in $\boldsymbol{s}$ may be formed with a mixing matrix A $(M \times K) : \boldsymbol{x} = A\boldsymbol{s}$. If the elements in A are linearly independent, then any signal source $\boldsymbol{s}_i$ can be recovered from $\boldsymbol{x}$ with a $\boldsymbol{W}_i$ matrix $(1 \times M) : \boldsymbol{s}_i = \boldsymbol{W}_i\boldsymbol{x}$. The desired solution here is to find an unmixing $\boldsymbol{W} = (W_1, W_2, \ldots, W_k)^{\boldsymbol{T}}$ so that each vector

value $\boldsymbol{W}_i$ recovers a different signal $\boldsymbol{y}_i$, where $\boldsymbol{y}_i$ is an estimated value of $\boldsymbol{s}_i$ source signal for signals $K = M$.

The method for recovering source signals is based on the following theory; the temporal predictability of a mixed signal $\boldsymbol{x}_i$ is usually lower than any of the source signals contributing to $\boldsymbol{x}_i$.

This parameter is used to define the temporal predictability measure $F(\boldsymbol{W}_i, \boldsymbol{x})$, which is used to estimate the relative predictability of a retrieved signal $\boldsymbol{y}_i$ by a matrix $\boldsymbol{W}_i$, where $\boldsymbol{y}_i = \boldsymbol{W}_i \boldsymbol{x}$. If signal sources are more predictable than the linear mixtures $\boldsymbol{y}_i$ of these signals, then the value of $\boldsymbol{W}_i$, which maximizes the predictability of an estimated signal $\boldsymbol{y}_i$, should produce a source signal [50]. The definition of predictability of an F signal is defined as:

$$F(\boldsymbol{W}_i, \boldsymbol{x}) = \log \frac{V(\boldsymbol{W}_i, \boldsymbol{x})}{U(\boldsymbol{W}_i, \boldsymbol{x})} = \log \frac{V_i}{U_i} = \log \frac{\sum_{\tau=1}^{n} (\overline{\boldsymbol{y_\tau}} - \boldsymbol{y_\tau})^2}{\sum_{\tau=1}^{n} (\widetilde{\boldsymbol{y_\tau}} - \boldsymbol{y_\tau})^2} \tag{16}$$

where $y_\tau = W_i x_\tau$ is the value of a signal y in time τ, and x_τ is a vector of K values of signal mixtures in time τ. The term U_i reflects the extent to which y_τ is provided by a short-term moving average $\widetilde{\boldsymbol{y_\tau}}$ of the values in y. On the contrary, the term V_i is a measure of the overall variability in y; therefore y_τ is provided by a long term moving average $\overline{\boldsymbol{y_\tau}}$ of the values in y. The predicted values $\widetilde{\boldsymbol{y_\tau}}$ and $\overline{\boldsymbol{y_\tau}}$ of y_τ are both exponentially weighted sums of measured signals until time $(\tau - 1)$, in such a way that the recent values have a coefficient greater than those in the distant past [50]:

$$\widetilde{\boldsymbol{y_\tau}} = \lambda_S \tilde{\boldsymbol{y}}_{(\tau-1)} + (1 - \lambda_S) \boldsymbol{y}_{(\tau-1)} \quad 0 \leq \lambda_S \leq 1 \tag{17}$$

$$\overline{\boldsymbol{y_\tau}} = \lambda_L \bar{\boldsymbol{y}}_{(\tau-1)} + (1 - \lambda_L) \boldsymbol{y}_{(\tau-1)} \quad 0 \leq \lambda_L \leq 1 \tag{18}$$

The half-life h_L of λ_L is much greater (typically 100 times greater) than the half-life h_L of λ_S. The relation between half-life h and parameter λ is defined as $\lambda = 2^{\frac{-1}{h}}$.

Note that maximizing only V_i would result in a high variance signal with no constraints on its temporal structure. In contrast, minimizing only U would result in a DC signal. In both cases, trivial solutions would be obtained for W_i because V_i can be maximized by setting the norm of W_i to be large, and U can be minimized by setting $W_i = 0$. In contrast, the ratio V_i/U_i can be maximized only if two constraints are both satisfied: (1) y has a nonzero range (i.e., high variance) and (2) the values in y change slowly over time. Note also that the value of F is independent of the norm of W_i, so that only changes in the direction of W_i affect the value of F [50].

If the value of F associated with a signal mixture x_i is not undefined, then the value of F of each mixture is greater than (or equal to) the value of F of each source signal in this mixture [50].

The half-life (h) determines the size of the moving averages h_L (long term moving average) and h_S (short term moving average). This half-life determines the number of elements that will be used to calculate the averages. A big half-life (h) determines a big λ, resulting in data with high correlation, but limits the sensitivity of individual or small variations in the signals. Whereas a small half-life (h) determines a small λ, resulting in data with minor correlation, with greater sensitivity of individual and small variations. Since the variable λ establishes the proportion that makes up the estimated values $\widetilde{\boldsymbol{y_\tau}}$ and $\overline{\boldsymbol{y_\tau}}$. They are the sum of the previous estimated average signals $\tilde{\boldsymbol{y}}_{(\tau-1)}$ and $\bar{\boldsymbol{y}}_{(\tau-1)}$ and previous estimated signals $\boldsymbol{y}_{(\tau-1)}$ as can be seen this relationship in Equations (17) and (18).

To estimate an individual signal, we should consider a scalar mixture signal y_i formed by the application of a matrix W_i, of $1 \times M$, to a set of signals x of $K = M$. Given that

$y_i = W_i x$, Equation (16) can be rewritten as:

$$F = \log \frac{W_i \bar{C} W_i^T}{W_i \tilde{C} W_i^T} \tag{19}$$

where $\bar{C}$ is a matrix of long-term covariances between signals and mixtures and $\tilde{C}$ is the matrix of short-term covariances. The long term covariance $\bar{C}_{ij}$ and the short-term covariance $\tilde{C}_{ij}$ among the mixtures are defined as:

$$\tilde{C}_{ij} = \sum_{\tau}^{n} (\boldsymbol{x}_{i\tau} - \tilde{\boldsymbol{x}}_{i\tau})(\boldsymbol{x}_{j\tau} - \tilde{\boldsymbol{x}}_{j\tau}) \tag{20}$$

$$\bar{C}_{ij} = \sum_{\tau}^{n} (\boldsymbol{x}_{i\tau} - \bar{\boldsymbol{x}}_{i\tau})(\boldsymbol{x}_{j\tau} - \bar{\boldsymbol{x}}_{j\tau}) \tag{21}$$

Note that $\tilde{C}$ and $\bar{C}$ need to be calculated only once for a given set of mixed signals and that the terms $(\boldsymbol{x}_{i\tau} - \bar{\boldsymbol{x}}_{i\tau})$ and $(\boldsymbol{x}_{i\tau} - \tilde{\boldsymbol{x}}_{i\tau})$ can be precalculated by using fast convolution operations [51].

The upward gradient F in relation to W_i can be used to maximize F, maximizing the predictability of y_i. The derivative of F in relation to W_i is:

$$\nabla \boldsymbol{W}_i F = \frac{2\boldsymbol{W}_i}{V_i} \bar{C} - \frac{2\boldsymbol{W}_i}{U_i} \tilde{C} \tag{22}$$

To estimate all sources simultaneously existent, the gradient of F is zero in the solution to Equation (22) [29,50]:

$$\boldsymbol{W}_i \bar{C} = \frac{V_i}{U_i} \boldsymbol{W}_i \tilde{C} \tag{23}$$

The extremes in F correspond to the values of W_i that satisfy Equation (23), which takes the form of the widespread problem of eigenvalues and eigenvectors [49]. The solutions for W_i can be obtained as eigenvectors of matrix $\left(\tilde{C}^{-1}\bar{C}\right)$, with corresponding eigenvalues $\gamma_i = \frac{V_i}{U_i}$. The results presented in this article were obtained using the *nonsymmetric eigenvalue* function of Matlab, being $\boldsymbol{W} = \boldsymbol{eig}\left(\bar{C}, \tilde{C}\right)$. All K signals can then be estimated by $y = Wx$, where each line of y corresponds to exactly one estimated signal y_i [50].

8. **Algorithm Performance Metric: Signal-Distortion Ratio (SDR) and Signal-to-Noise Ratio (SNR).** The method presented will be applied in 2 performance measures, SDR (signal-distortion rate) and SNR (signal-to-noise ratio) [36]. The algorithms used as metrics to evaluate the results can be applied to all the BSS problems. The mixing system and the unmixing technique do not need to be known.

Performance measures are found for each estimated $\hat{S}_j$ comparing them with a given original source S_j. If necessary, $\hat{S}_j$ can be compared with all sources $(S_{j'})$ $1 \leq j' \leq n$ and the original sources can be selected as those that present the best results.

The calculation of the criteria involves two successive stages. In the first stage, the estimated signal $\hat{S}_j$ is decomposed as Equation (24),

$$\hat{S}_j = S_{target} + e_{interf} + e_{noise} + e_{artif} \tag{24}$$

where $S_{target} = f(S_j)$ is a version of S_j modified by a distortion allowed $f \in F$ (where F is a set of distortions), and where e_{interf}, e_{noise} and e_{artif} are, respectively, interference, noise, and artifact errors. These four terms represent the part of $\hat{S}_j$ perceived as coming from the desired source S_j, from other unwanted sources $(S_{j'})$ $j' \neq j$, and from noise (V_i)

$1 \leq i \leq m$ [36]. In the second stage, the energy rates to evaluate each one of these four terms are calculated.

A performance criterion for the most common case was proposed, when the distortions allowed in Y_n are invariant in time. First, we show how to decompose Y_n into four terms as in Equation (24), and then we define the relevant energy rates between those terms.

When A is an instant time invariant matrix and when the mixture is separated using an instant time invariant matrix W, $\hat{S}_j$ can be decomposed as,

$$\hat{S}_j = (WA)_{jj} S_j + \sum_{j' \neq j} (WA)_{jj'} S_{j'} + \sum_{i=1}^{m} W_{ji} V_i \tag{25}$$

Since $(WA)_{jj}$ is a time invariant gain, it seems natural to identify the three terms of this sum as S_{target}, e_{interf} and e_{noise}, respectively (e_{artif} is zero here). However, Equation (25) cannot be used as a definition of S_{target}, e_{interf}, e_{noise}, and e_{artif} since the mixing and unmixing systems are not known. Also, the first two terms of Equation (25) cannot be perceived as separate objects when an unwanted source $S_{j'}$ is highly correlated with the desired source S_j.

With that, the proposed decomposition is based on the orthogonal projection. Let us denote $\prod\{y_1, \ldots, y_k\}$ the orthogonal projector onto the subspace generated by vectors $y_1, \ldots, y_k$. The projector is a matrix $T \times T$, where T is the size of these vectors. We consider three orthogonal projectors [36]:

$$P_{S_j} := \prod\{S_j\} \tag{26}$$

$$P_S := \prod\{(S_{j'}) 1 \leq j' \leq n\} \tag{27}$$

$$P_{S,V} := \prod\{(S_{j'}) 1 \leq j' \leq n, (V_i) 1 \leq i \leq m\} \tag{28}$$

The estimated sources $\hat{S}_j$ are decomposed as the sums of four terms [36]:

$$S_{target} := P_{S_j} \hat{S}_j \tag{29}$$

$$e_{interf} := P_S \hat{S}_j - P_{S_j} \hat{S}_j \tag{30}$$

$$e_{noise} := P_{S,V} \hat{S}_j - P_S \hat{S}_j \tag{31}$$

$$e_{artif} := \hat{S}_j - P_{S,V} \hat{S}_j \tag{32}$$

The calculation of S_{target} is direct as long as it involves only a simple integer product: $S_{target} = \langle \hat{S}_j, S_j \rangle S_j / ||S_j||^2$. The calculation of e_{artif} is a bit more complex. If the sources are mutually orthogonal, then $e_{artif} = \sum_{j' \neq j} \langle \hat{S}_j, S_{j'} \rangle S_{j'} / ||S_{j'}||^2$. On the other hand, if you use a vector of coefficients $\boldsymbol{C}$ such that $P_S \hat{S}_j = \sum_{j'=1}^{n} \bar{\boldsymbol{C}}_{j'} S_{j'} = \boldsymbol{C}^H S$ (where $(.)^H$ denotes a Hermitian transpose), then $\boldsymbol{C} = \boldsymbol{R}_{SS}^{-1} \left[\langle \hat{S}_j, S_1 \rangle, \ldots, \langle \hat{S}_j, S_n \rangle \right]^H$, where $\boldsymbol{R}_{SS}$ is the Gram matrix of sources defined by $(\boldsymbol{R}_{SS})_{jj'} = \langle S_j, S_{j'} \rangle$. The calculation of $P_{S,V}$ proceeds in a similar way. However, most of the time we can assume that the noise signals are mutually orthogonal and orthogonal to each source, so that $P_{S,V} \hat{S}_j \approx P_S \hat{S}_j + \sum_{i=1}^{m} \langle \hat{S}_j, V_i \rangle V_i / ||V_i||^2$ [36].

Starting from the decomposition of $\hat{S}_j$ of Equations (26) to (32), we can define numeric performance criteria for the calculation of energy rates expressed in decibels. We define signal-distortion rate as [36]:

$$SDR = 10 \log_{10} \frac{||S_{target}||^2}{||e_{interf} + e_{noise} + e_{artif}||^2} \tag{33}$$

the signal-to-noise rate [36]:

$$SNR = 10 \log_{10} \frac{||S_{target} + e_{interf}||^2}{||e_{noise}||^2} \tag{34}$$

9. **Algorithm Performance Metric: Signal Interference Ratio (SIR).** To evaluate the algorithm used in this work, we applied signal-interference ratio (SIR) [35], described below. The input *SIR*, SIR^{in}, measures the performance of mixed signals before they are processed by the proposed BSS architecture. Being x_i the observation of channel i with Equation (35),

$$x_i = \sum_{j=1}^{n} a_{i,j} s_j + v_i \tag{35}$$

where $a_{i,j}$ denotes the coefficients of mixtures, s_j is the original source, v_i denotes noise, and m is the number of sources. SIR^{in} calculates the rate of k's source signals $a_{i,k} s_k$ as observed in Equation (36),

$$SIR_k^{in}(i) = 10 \log_{10} \frac{a_{i,k}^2 ||s_k||^2}{||x_i - a_{i,j} s_k||^2} \tag{36}$$

When all n samples are considered, the maximum SIR_k^{in} is defined by Equation (37) [35],

$$SIR_k^{in} = \max_{i=1,\ldots,n} SIR_k^{in}(i) \tag{37}$$

The same approach is used to set the output *SIR*, SIR^{out}. Being $\hat{A}_o$ and $\hat{S}_o$, respectively, the mixing matrix and the signals fonts derived from the BSS method; and being, A and S, the real matrix mixing and signal sources, respectively. The order of the signal sources estimated at $\hat{S}_o$ can be changed to correspond in S to solve the following optimization problem,

$$P_o = \arg\min_P ||S - P^T \hat{S}_o||_F^2 \tag{38}$$

where P is a permutation matrix. So, $\hat{A} = \hat{A}_o P_o$ and $\hat{S} = P_o^T \hat{S}_o$ is defined as estimated mixing matrix and source signals respectively. SIR^{out} calculates the rate of k's signals $a_{i,k} s_k$ derived from the BSS solution as Equation (39) [35],

$$SIR_k^{out}(i) = 10 \log_{10} \frac{a_{i,k}^2 ||s_k||^2}{||a_{i,k} s_k - \hat{a}_{i,j} \hat{s}_k||^2} \tag{39}$$

where $\hat{a}_{i,j}$ and $\hat{s}_k$ are $a_{i,j}$ and s_k estimated in $\hat{A}$ and $\hat{S}$, respectively. The maximum output *SIR* for a source signal k is defined as,

$$SIR_k^{out} = \max_{i=1,\ldots,n} SIR_k^{out}(i) \tag{40}$$

Therefore, the *SIR* for source signal k is,

$$SIRI_k = SIR_k^{out} - SIR_k^{in} \tag{41}$$

and the average *SIR* for all strong signals is [35],

$$SIRI = \frac{1}{m} \sum_{k=1}^{m} SIRI_k \tag{42}$$

For the analysis of this work Equations (37), (40) and (42) are evaluated, since they establish the maximum signal-interference ratios of inputs before passing by the BSS and estimated signals after processing of the BSS, and the average rate.

10. **Signal Analysis.** Initially, a verification of the signal given by the proposed BSS was made, then identified as noise and if it has a Gaussian probability density function (PDF) [52], because this type of function is characteristic of noise. This hypothesis was confirmed as really being a Gaussian PDF. Figure 7 shows the probability density function of the error determined by the BSS proposed in Figure 5.

Table 2 shows the convergence rates between the signals of Gauges 1 and 2. This rate was determined by comparing the original signals, and after the original signals after the application of the BSS proposed.

Table 3 identifies the values determined by the metrics of performance [35,36] comparing the original signals with the proposed architecture.

Table 4 describes the results for the measurements of signal-distortion ratio (SNR), signal-to-noise ratio (SNR) [36] and signal-interference ratio (SIR) [35] of the second set of signals analyzed [34].

Table 5 shows the result of the convergence between the signals, where the difference between the points of the signal from the proposed BSS and the numerical model is much smaller than the difference of the experimental and the numerical signal.

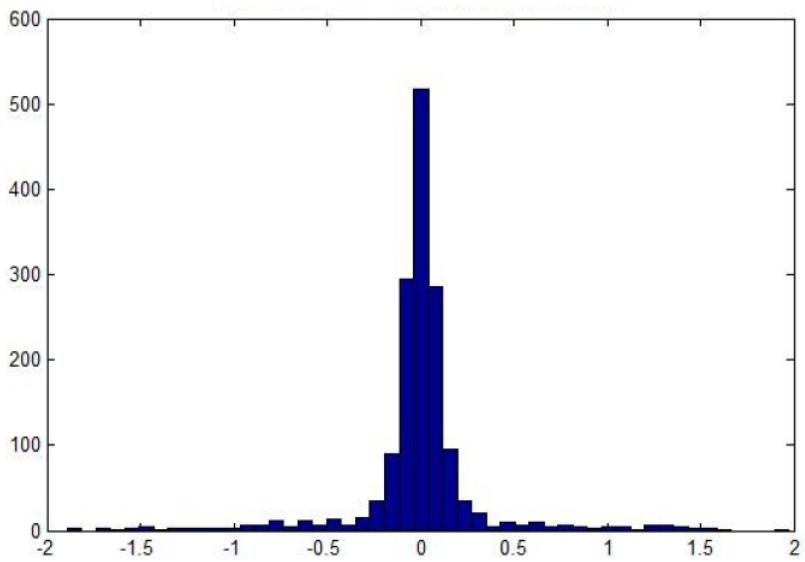

FIGURE 7. Behavior of the probability density function of the noise shown in Figure 5

TABLE 2. Convergence rate of signals (Gauges 1 and 2) – analysis between original signals – analysis between proposed algorithm signals

Test Number	Signal Convergence (%)	
	Between Original Signals	Between Proposed Algorithm Signals
Test 1	17	83
Test 2	18	82
Test 3	18	82
Test 4	16	84
Test 5	14	86
Test 6	9	91

TABLE 3. Metrics between proposed algorithm values and original values of the first set of signals

Test Number	Metrics between the Proposed Algorithm Signals and Original Signals						
		Maximum Signal-To-Noise Ratio			Temporal Predictability		
		SNR	SDR	SIR	SNR	SDR	SIR
Test 1	Strain Gauge 1	12.3	12.3	3.45	10.55	10.55	2.52
	Strain Gauge 2	12.4	12.4	3.51	10.56	10.56	2.58
Test 2	Strain Gauge 1	11.82	11.82	3.10	10.65	10.65	2.62
	Strain Gauge 2	11.77	11.77	3.03	10.62	10.62	2.58
Test 3	Strain Gauge 1	11.08	11.08	2.96	10.55	10.55	2.53
	Strain Gauge 2	11.04	11.04	2.91	10.44	10.44	2.49
Test 4	Strain Gauge 1	11.52	11.52	3.01	10.11	10.11	2.35
	Strain Gauge 2	11.47	11.47	2.96	10.07	10.07	2.30
Test 5	Strain Gauge 1	10.98	10.98	2.89	10.28	10.28	2.41
	Strain Gauge 2	11.12	11.12	2.93	10.31	10.31	2.48
Test 6	Strain Gauge 1	11.72	11.72	3.08	9.58	9.58	2.25
	Strain Gauge 2	11.64	11.64	3.02	9.52	9.52	2.20
Average		11.57		3.07	10.27		2.44

TABLE 4. Performance measurements: signal distortion ratio, signal noise ratio and signal interference ratio – signals of the experimental and numerical models

Performance Measurements (dB): SDR and SNR				
	Maximum Signal-To-Noise Ratio		Temporal Predictability	
	Proposed Algorithm – Experimental	Proposed Algorithm – Numerical	Proposed Algorithm – Experimental	Proposed Algorithm – Numerical
SDR	10.961010	11.032002	5.566444	6.051403
SNR	10.961098	11.032089	5.566497	6.051485
SIR	2.99	3.81	1.78	1.97

TABLE 5. Convergence rate between experimental – numerical signals and proposed algorithm – numerical signals

Convergence between the Signals (%)	
Experimental Signal Numerical Signal	Proposed Algorithm Signal Numerical Signal
11	89

11. **Conclusions.** We conclude, analyzing Figure 7, which represents the probability density function (PDF) of the noise found by proposed algorithm, that this function really is a Gaussian distribution. Therefore, it is characterized as a noise distribution [52].

We concluded that the proposed algorithm performs as expected. Performance metrics (Table 3) were compatible with the theoretical noise levels (Table 1) indicated initially in

the experimental simulations. This proves that the proposed algorithm can detect the different noise levels and establish a true relation with the rates determined by performance metrics.

Table 2 shows the convergence rates between the original signals and the signals after being processed by proposed algorithm. We must point out that different noise levels were inserted in the two sensors used to monitor deformation of the same point. Analyzing the rates it is possible to confirm that the percentage of convergence between the signals after the application of the proposed algorithm is much higher. This shows greater noise reduction in the signals, because without the presence of any kind of noise the signals would be exactly the same (convergent).

The convergence rate between the signal of the proposed algorithm and the numerical model was much larger than between the experimental signal and the numerical model. This shows that there is noise, identified by the proposed algorithm, which came from the signal acquisition, as shown in Table 5.

When analyzing the SDR and SNR measurements, we realize that there was a significant difference. Besides this, there was a gain of almost 4 dB in the proposed algorithm signal in relation to the experimental signal, thus, significantly reducing the level of noise in the signal, confirming the efficiency of the proposed algorithm. The slight difference between SNR and SDR is due to the fact that the component for the e_{artif} measure is small. The final noise level that was 10^{-7} [45], specified by the equipment utilized, went to around 10^{-11} after the application of the proposed algorithm.

The SIR metric also accompanies the development of other metrics (SNR and SDR), determining values between 3 and 4 dBs. This metric performs the calculations between the SIR^{in} (input-signal) and SIR^{out} (output - proposed algorithm signal), which represents the difference between the two levels of noise.

The efficiency of the maximum signal-to-noise ratio algorithm is evident when compared with the other algorithm used by the proposed algorithm. The temporal predictability algorithm presented values of metrics of performance below those determined by maximum signal-to-noise ratio.

The objectives of the proposed algorithm were achieved successfully based on the numerical parameters found in the simulations. With that, this algorithm is a great solution for noise reduction in signals monitored by electronic equipment. Another advantage of this algorithm is the fact that it can be used in any application of noise reduction. This is because it does not rely on prior information from the monitored signals, and works with one or more input signals.

As a future proposal, it would be interesting to carry out the study of this algorithm in signals from sensors more sensitive to noise. The characterization of thermal profiling in wells would be a very interesting application for the algorithm proposed in this work.

REFERENCES

[1] G. Nery, Monitoreo em la construcción civil - Boletn técnico, Asociación Latinoamericana de Control de Calidad, Patología y Recuperación de la Construcción - *ALCONPAT Int.*, p.18, 2013.

[2] T. F. Collura, History and evolution of electroencephalographic instruments and techniques, *Clinical Neurophysiology*, vol.10, no.4, pp.476-504, 1993.

[3] B. He, G. Lu, K. Chu and G. Ma, Developing of high accuracy and low capacity strain gage based load cell for electronic scale, *The 9th International Conference on Electronic Measurement & Instruments*, vol.10, pp.552-556, 2009.

[4] M. Romanzini, E. L. Petroski and F. F. Reichert, Accelerometers thresholds to estimate physical activity intensity in children and adolescentes: A systematic review, *Revista brasileira de cineantropometria e desenvolvimento humano*, vol.14, no.1, pp.101-113, 2012.

[5] K. Bethe, The scope of the strain gage principle, *VLSI and Computer Peripherals Microelectronic Applications in Intelligent Peripherals and Their Interconnection Networks*, Hamburg, Germany, pp.31-38, 1989.
[6] F. F. M. Santos, *Uso de extensômetro para altas temperaturas na estimativa de vida residual - monitoração em tempo real das deforma ções de tubulações em usinas de geração trmica*, Dissertação (mestrado em Engenharia Metalúrgica e de Materiais) - Universidade Federal do Rio de Janeiro, Rio de Janeiro, RJ, 2011.
[7] B. Studyvin, R. L. Doty and R. Repplinger, Temperature effects on strain gages used on aerospace nickel hydrogen batteries, *Battery Conference on Applications and Advances*, Long Beach, CA, USA, pp.325-328, 1999.
[8] L. Picciano and J. K. J. Li, A novel strain gage transducer design for biomedical applications, *Engineering in Medicine and Biology Society*, vol.12, no.2, pp.512-513, 1990.
[9] J. E. Ramus, Radiation induced electrical transients in strain gage and temperature transducer circuits in a pulsed reactor environment, *Nuclear Science*, vol.11, no.5, pp.111-122, 1964.
[10] O. T. Gregory and X. Chen, A low TCR nanocomposite strain gage for high temperature aerospace applications, *Sensors*, pp.624-627, 2007.
[11] S. Poussier, H. Rabah and S. Weber, Design and implementation of a smart strain gage conditioner, *International Workshop on Computer Architectures for Machine Perception*, pp.184-192, 2003.
[12] C. R. Shearer, Temperature compensation of transducers using semiconductor strain gages, *Trans. Aerospace*, vol.3, no.2, pp.53-59, 1965.
[13] V. C. M. N. Leite, *Separação cega de sinais: Análise comparativa entre algoritmos*, Dissertação (Mestrado em Engenharia Elétrica) - Universidade Federal de Itajubá, Itajubá, Minas Gerais, 2004.
[14] C. R. Farrar and K. Worden, An introduction to structural health monitoring, *Philosophical Transactions of the Royal Society*, vol.365, no.1851, pp.303-315, 2006.
[15] V. Zarzoso and A. K. Nandi, Noninvasive fetal electrocardiogram extraction: Blind separation versus adaptive noise cancellation, *IEEE Trans. Biomedical Engineering*, vol.48, no.1, 2001.
[16] J. V. Stone, Independent component analysis: An introduction, *Trends in Cognitive Sciences*, vol.6, no.2, 2002.
[17] T. He, G. Clifford and L. Tarassenko, Application of independent component analysis in removing artefacts from the electrocardiogram, *Neural Comput. & Applic.*, vol.15, pp.105-116, 2006.
[18] M. Ferdjallah and R. E. Barr, Adaptive digital notch filter design on the unit circle for the removal of powerline noise from biomedical signals, *IEEE Trans. Biomedical Engineering*, vol.41, no.6, 1994.
[19] E. A. Clansy, E. L. Morin and R. Merletti, Sampling, noise-reduction and amplitude estimation issues in surface electromyography, *Journal of electromyography and Kinesiology*, no.12, pp.1-16, 2002.
[20] H. H. Asada, H. H. Jiang and P. Gibbs, Active noise cancellation using MEMS accelerometers for motion-tolerant wearable bio-sensors, *Proc. of the 26th Annual International Conference of the IEEE EMBS*, San Francisco, CA, USA, pp.1-5, 2004.
[21] P. C. Chang, A. Flatau and S. C. Liu, Review paper: Health monitoring of civil structure, *Structure Health Monitoring*, 2010.
[22] F. Odille, C. Pasquier, R. Abacherli, P. A. Vuissoz, G. P. Zientara and J. Felblinger, Noise cancellation signal processing method and computer system for improved real-time electrocardiogram artifact correction during MRI data acquisition, *IEEE Trans. Biomedical Engineering*, vol.54, no.4, 2007.
[23] K. Mine and Y. Morimoto, Methods of alternating noise canceling for an instrumentation using strain gages, *IEEE Trans. Industrial Electronics*, vol.37, no.3, pp.250-252, 1990.
[24] B. Peeters and G. De Roeck, Stochastic system identification for operational modal analysis: A review, *J. Dyn. Syst. Meas. Control*, vol.123, no.4, pp.659-667, 2001.
[25] A. Cichocki and S. I. Amari, *Adaptive Blind Signal and Image Processing: Learning Algorithms and Applications*, John Wiley & Sons, 2002.
[26] A. Hyvarinen, Survey on independent component analysis, *Neural Computing Surveys*, vol.2, pp.94-128, 1999.
[27] S. A. C. Alvarez, *Una visión unificada de los algoritmos de separacióniegа de fuentes*, Tese (Doutorado em Engenharia Elétrica), Universidade de Vigo, 1999.
[28] D. C. B. Chan, *Blind Signal Separation*, Ph.D. Thesis, Signal Processing and Communications Lab, Department of Engineering, University of Cambridge, UK, 1997.
[29] J. Ma and X. Zhang, Blind source separation algorithm based on maximum signal noise ratio, *The 1st International Conference on Intelligent Networks and Intelligent Systems*, pp.625-628, 2008.

[30] P. Comon and C. Jutten, *Handbook of Blind Separation – Independent Component Analysis and Applications*, Elsevier, 2009.
[31] A. Havarinen and E. Oja, Independent component analysis: Algorithms and applications, *Neural Networks*, vol.13, pp.411-430, 2000.
[32] C. C. S. Almeida, *Análise de técnicas separação cega de fontes para remoção de artefatos em interfaces cérebro-máquina*, Dissertação (mestrado em Engenharia da Informação) – Universidade Federal do ABC, Santo André, São Paulo, 2013.
[33] A. A. Filho, *Elementos finitos - a base da tecnologia*, Editora Érica, Rio de Janeiro, 2005.
[34] G. V. Nunes, *Análise numérica paramétrica de ligações tipo "T", "K" e "TK" compostas por perfis tubulares de seção retangular e circular*, Dissertação (Mestrado em Engenharia Civil) – Universidade de Ouro Preto, Ouro Preto, Minas Gerais, 2012.
[35] W. L. Hwang and J. Ho, Null space component analysis for noisy blind source separation, *Signal Processing*, vol.109, pp.301-316, 2015.
[36] E. Vicente, R. Gribonval and C. Fvotte, Performance measurement in blind audio source separation, *IEEE Trans. Audio, Speech, and Language Processing*, vol.14, no.4, pp.1462-1469, 2006.
[37] B. P. Lathi, *Modern Digital and Analog Communication Systems*, 3rd Edition, Oxford University Press, New York, 1998.
[38] A. P. Silva, *Separação cega de misturas convolutivas no domínio do tempo utilizando clusterização*, Dissertação (mestrado em Eletrnica e Computação) – Universidade Federal do Rio de Janeiro, Rio de Janeiro, RJ, 2009.
[39] L. Yang and Z. Ming, Blind source separation based on fastICA, *The 9th International Conference on Hybrid Intelligent Systems*, vol.2, pp.475-479, 2009.
[40] A. Bell and T. J. Sejnowski, An information maximization approach to blind separation and deconvolution, *Neural Computing*, vol.7, no.6, pp.1129-1159, 1995.
[41] A. Hyvarinen, J. Karhunen and E. Oja, *Independent Component Analysis*, J. Wiley, New York, 2001.
[42] J. F. Cardoso, A blind beam-forming for non-Gaussian signals, *IEEE Proc. Part F – Radar and Signal Processing*, vol.140, no.6, pp.362-370, 1993.
[43] A. Hyvarinen, Gaussian moments for noisy independent component analysis, *IEEE Signal Processing Letters*, vol.6, no.6, pp.145-147, 1999.
[44] HBM, *Data Sheet: Spider 8*, 2012.
[45] HBM, *Data Sheet: Quatum X MX840B*, 2015.
[46] M. V. Exter, Noise and signal processing, *Extra Syllabus for (Third-Year) Course*, Universiteit Leiden, 2003.
[47] F. C. Simões, *Estudo da relação sinal - ruído na aquisição de dados de sensores de alta impedância*, Dissertação de graduação, Universidade Estadual de Campinas, 2008.
[48] A. A. Farias, J. F. Soares and C. C. Csar, Introdução à Estatstica, Editora LTC, Rio de Janeiro, 1998.
[49] M. Borga, Learning multidimensional signal processing, *International Conference on Pattern Recognition*, 1998.
[50] J. V. Stone, Blind source separation using temporal predictability, *Neural Computation*, vol.13, pp.1559-1574, 2001.
[51] S. Eglen, A. Bray and J. Stone, Unsupervised discovery of invariances, *Network: Comput. Neural Syst.*, vol.8, pp.441-452, 1997.
[52] W. F. Lages, *Probabilidade e variveis aleatórias*, Departamento de engenharia elétrica, Universidade federal do rio grande do sul, 2004.